Nuclear Orphan Receptor TAK1/TR4-Deficient Mice Are Protected Against Obesity-Linked Inflammation, Hepatic Steatosis, and Insulin Resistance

Hong Soon Kang,[1] Kyoko Okamoto,[1] Yong-Sik Kim,[1] Yukimasa Takeda,[1] Carl D. Bortner,[2] Huaixin Dang,[1] Taira Wada,[3] Wen Xie,[3] Xiao-Ping Yang,[1] Grace Liao,[1] and Anton M. Jetten[1]

OBJECTIVE—The nuclear receptor TAK1/TR4/NR2C2 is expressed in several tissues that are important in the control of energy homeostasis. In this study, we investigate whether TAK1 functions as a regulator of lipid and energy homeostasis and has a role in metabolic syndrome.

RESEARCH DESIGN AND METHODS—We generated TAK1-deficient ($TAK1^{-/-}$) mice to study the function of TAK1 in the development of metabolic syndrome in aged mice and mice fed a high-fat diet (HFD). (Immuno)histochemical, biochemical, and gene expression profile analyses were performed to determine the effect of the loss of TAK1 expression on lipid homeostasis in liver and adipose tissues. In addition, insulin sensitivity, energy expenditure, and adipose-associated inflammation were compared in wild-type (WT) and $TAK1^{-/-}$ mice fed a HFD.

RESULTS—TAK1-deficient ($TAK1^{-/-}$) mice are resistant to the development of age- and HFD-induced metabolic syndrome. Histo- and biochemical analyses showed significantly lower hepatic triglyceride levels and reduced lipid accumulation in adipose tissue in $TAK1^{-/-}$ mice compared with WT mice. Gene expression profiling analysis revealed that the expression of several genes encoding proteins involved in lipid uptake and triglyceride synthesis and storage, including Cidea, Cidec, Mogat1, and CD36, was greatly decreased in the liver and primary hepatocytes of $TAK1^{-/-}$ mice. Restoration of TAK1 expression in $TAK1^{-/-}$ hepatocytes induced expression of several lipogenic genes. Moreover, $TAK1^{-/-}$ mice exhibited reduced infiltration of inflammatory cells and expression of inflammatory genes in white adipose tissue, and were resistant to the development of glucose intolerance and insulin resistance. $TAK1^{-/-}$ mice consume more oxygen and produce more carbon dioxide than WT mice, suggesting increased energy expenditure.

CONCLUSIONS—Our data reveal that TAK1 plays a critical role in the regulation of energy and lipid homeostasis, and promotes the development of metabolic syndrome. TAK1 may provide a new therapeutic target in the management of obesity, diabetes, and liver steatosis. ***Diabetes*** **60:177–188, 2011**

From the [1]Cell Biology Section, Laboratory of Respiratory Biology, National Institute of Environmental Health Sciences, National Institutes of Health, Research Triangle Park, North Carolina; the [2]Laboratory of Signal Transduction, Division of Intramural Research, National Institute of Environmental Health Sciences, National Institutes of Health, Research Triangle Park, North Carolina; and the [3]Center for Pharmacogenetics and Department of Pharmaceutical Sciences, University of Pittsburgh, Pittsburgh, Pennsylvania.

Corresponding author: Anton M. Jetten, jetten@niehs.nih.gov.

Received 4 May 2010 and accepted 14 September 2010. Published ahead of print at http://diabetes.diabetesjournals.org on 23 September 2010. DOI: 10.2337/db10-0628.

Obesity is a major health-care concern in Westernized cultures that affects ~30% of the general population in the U.S. (1,2). A strong etiologic link has been found between obesity and several obesity-associated diseases, including insulin-resistance, type 2 diabetes, cardiovascular disease, and nonalcoholic fatty liver disease. There is considerable evidence indicating that systemic low-grade inflammation associated with obesity plays a pivotal role in the pathogenesis of metabolic syndrome (3–6). In particular, the infiltration of macrophages and T lymphocytes in hypertrophic adipose tissue and the production of proinflammatory cytokines are important early events in the development of obesity-associated complications (6–9).

TAK1 (TR4, NR2C2), together with the closely related transcription factor TR2 (NR2C1), form a subclass of the nuclear receptor superfamily (10–12). TAK1 is highly expressed in several tissues, including the testis, brain, kidney, liver, and adipose tissue. Although TAK1 is still considered to be an orphan receptor, recent reports suggest that certain fatty acids and eicosanoids bind to and enhance the transcriptional activity of TAK1, thereby suggesting that TAK1 might function as a lipid sensor (13,14). Although the precise physiologic functions of TAK1 remain poorly understood, characterization of TAK1-deficient mice have suggested a role for TAK1 in cerebellar development and reproductive functions (15–18). More recent studies have provided evidence suggesting a role for TAK1 in lipid metabolism and gluconeogenesis (14,19–21).

In the present study, we used a TAK1-deficient ($TAK1^{-/-}$) mouse model to obtain further insights into the physiologic roles of TAK1 in energy homeostasis. We show, for the first time, that male $TAK1^{-/-}$ mice are resistant to the development of age- and high-fat diet (HFD)-induced obesity and are protected against obesity-linked hepatic steatosis, white adipose tissue (WAT)-associated inflammation, and insulin resistance. Our study reveals that the TAK1-signaling pathway plays a critical role in the regulation of lipid and energy homeostasis and metabolic syndrome. Because TAK1 functions as a ligand-dependent transcription factor, it may provide a novel therapeutic target in the management and prevention of obesity and associated pathologies.

RESEARCH DESIGN AND METHODS

$TAK1^{-/-}$ mice. A schematic view and detailed information on the knockout strategy and mice are provided in supplementary Fig. 1 in the online appendix available at http://diabetes.diabetesjournals.org/cgi/content/full/db10-0628/DC1. $TAK1^{-/-}$ mice were bred into a C57BL/6 background for

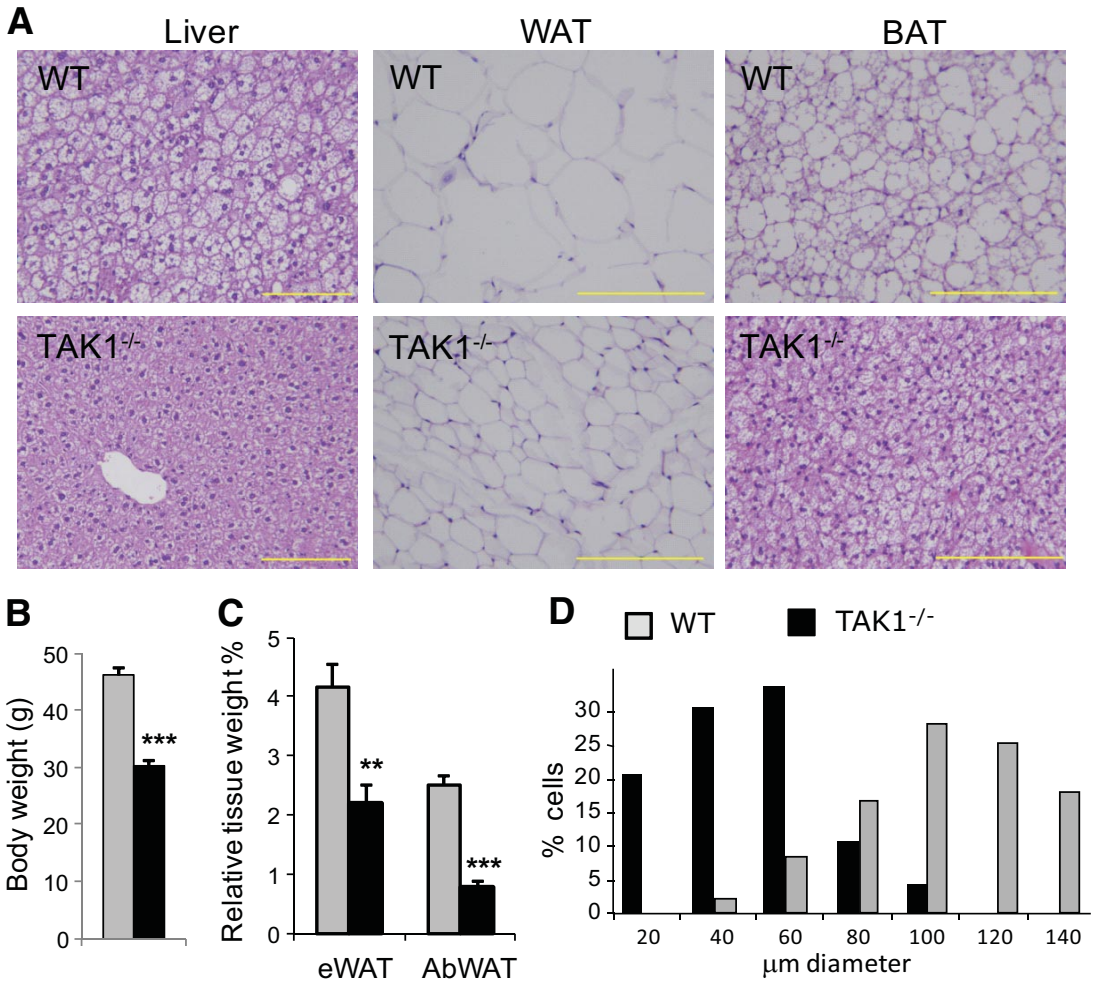

FIG. 1. TAK1$^{-/-}$ mice are resistant to age-induced hepatic steatosis and display a reduced adiposity. *A*: Representative hematoxylin and eosin (H&E) staining of sections of liver, WAT, and BAT from 1-year-old WT and TAK1$^{-/-}$ male mice. Scale bar indicates 250 μm. *B*: One-year-old male TAK1$^{-/-}$ mice fed a normal diet have a reduced total body weight compared with littermate WT controls. *C*: Relative weights of epididymal (eWAT) and abdominal (AbWAT) WAT of WT and TAK1$^{-/-}$ mice. *D*: Comparison of the cell size of WAT adipocytes from 1-year-old WT and TAK1$^{-/-}$ male mice. Cell diameters (n = 100) were measured and the percentages of different size cells calculated and plotted. (A high-quality color representation of this figure is available in the online issue.)

>8 generations. Mice were supplied ad libitum with National Institutes of Health-A31 formula and water. Mice that were 8 to 12 weeks old were fed a high-fat diet (HFD; D12492, Research Diets, New Brunswick, NJ) for 6 weeks, unless indicated otherwise. All animal protocols followed the guidelines outlined by the National Institutes of Health Guide for the Care and Use of Laboratory Animals and were approved by the Institutional Animal Care and Use Committee at the National Institute of Environmental Health Sciences.

Cell culture and viral infection. Primary hepatocytes were isolated using a Hepatocyte Isolation System (Worthington Biomedical, Lakewood, NJ). To generate adenovirus, TAK1WT and TAKΔAF2, a mutant lacking the AF2 domain, were cloned to pShuttle-IRES-hrGFP-1 vector and then transferred into AdEasy-1 (Stratagene, LA Jolla, CA). Adenovirus was then generated according to the manufacturer's protocol. Hepa1–6/Emp, Hepa1–6/TAK1, and Hepa1–6/TAKΔAF2 cells were generated by infection with retrovirus containing the empty vector pLXIN, pLXIN-TAK1, or pLXIN-TAK1ΔAF2, respectively. After selection in G418, separate clones were isolated. All cells were maintained in Dulbecco's modified Eagle's medium containing 10% FBS.

Histology and immunostaining. Adipose and liver specimens (n = 6) were fixed in 4% paraformaldehyde, paraffin-embedded, and tissue sections (5 μm) stained with hematoxylin-esosin. The average diameter of white adipocytes was calculated from 20–30 cells/field and 3 fields/section. For the detection of macrophages, sections of white adipose tissue (WAT) were stained with an F4/80 antibody (Santa Cruz, CA) and avidin-biotin-peroxidase detection system.

RNA isolation, microarray analysis, and QRT-PCR. RNA isolation, microarray analysis, and QRT-PCR were carried out as described previously (22). Total RNA from individual mice (n = 4–10) in each group was analyzed as indicated. Details are listed in supplementary Table 1.

Biochemical assays. Blood levels of free fatty acids, β-hydroxybutyrate, glucose, cholesterol, triglycerides, and HDL were determined using the Cobas Mira Classic Chemistry System (Roche Diagnostics Systems, Montclair, NJ). The chemical reagents for all assays were purchased from Equal Diagnostics (Exton, PA). Serum insulin levels were analyzed with an insulin radioimmunoassay kit (Millipore, St. Charles, MO). To measure liver lipid content, tissues were homogenized and lipids extracted as previously described (23). Triglyceride and cholesterol levels were measured with Stanbio assay kits (Stanbio Laboratory, Boerne, TX). Total ketones were analyzed with an Autokit (Waco Chemical GmbH, Neuss, Germany).

Metabolic analysis. Wild-type (WT) and TAK1$^{-/-}$ mice were fed either a normal diet or HFD for 18 weeks and their oxygen consumption, CO_2 production, and respiratory exchange ratio were analyzed with a LabMaster system (TSE Systems, Chesterfield, MO). All values were measured every 5 min for 3 days. The average of the values during the circadian time or light period and dark period were calculated and presented. P values were calculated using the Student t test.

Isolation of the stromal-vascular fraction and flow cytometry analysis. Stromal-vascular fraction (SVF) was isolated from epididymal white adipose tissue (eWAT) of mice fed with a HFD for 18 weeks and analyzed by flow cytometry with anti-F4/80 antibody (Invitrogen, Camarillo, CA), and anti-CD3, CD4, CD8, and CD11b antibodies (BD Biosciences, San Jose, CA) as described (6). Cells were costained with 7-amino-actinomycin D (7-AAD) or propidium iodine to exclude dead cells. Cells were analyzed with a BD LSR II Flow cytometer (Becton Dickinson) using FACSDiVa software as previously described (6).

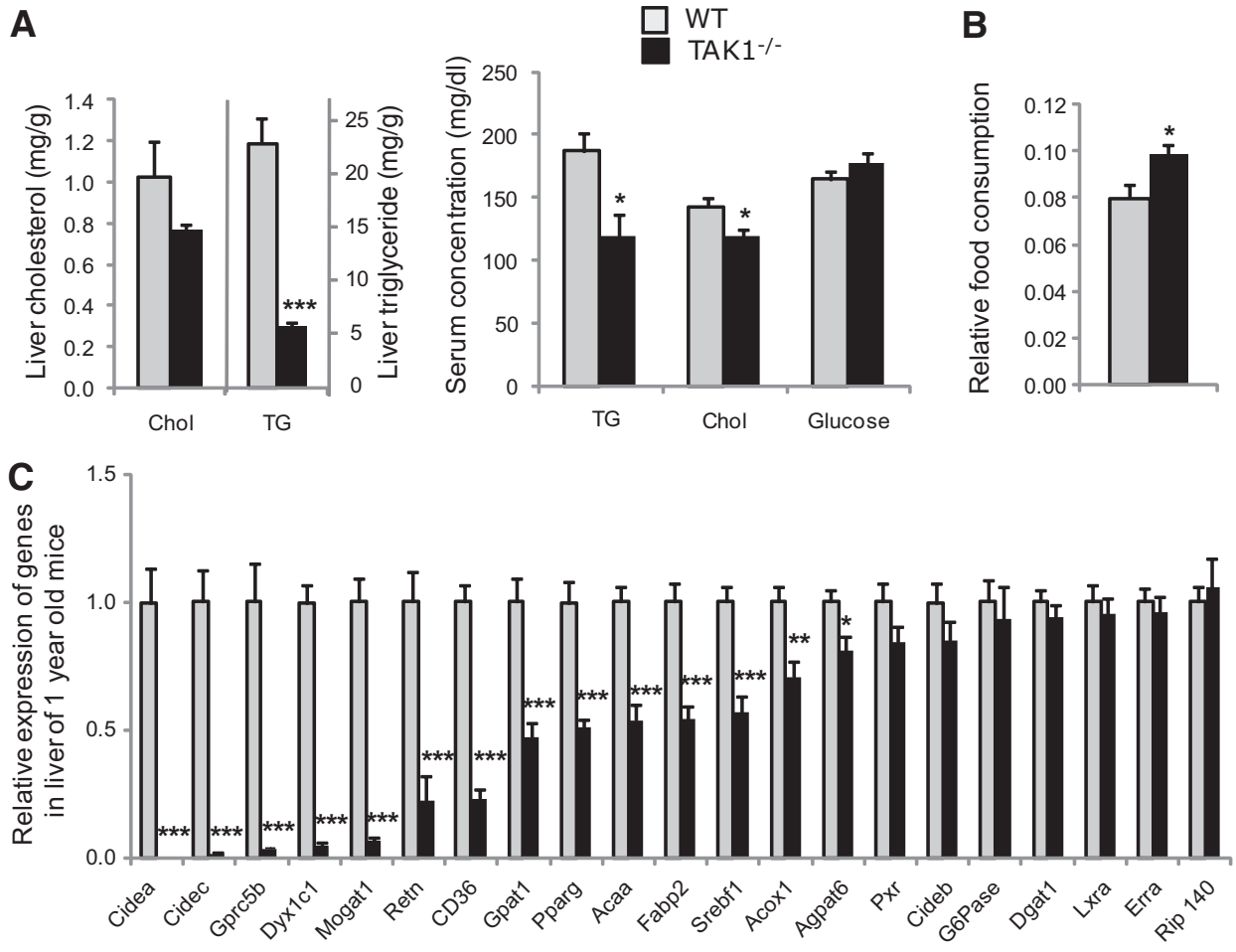

FIG. 2. Reduced lipid accumulation and lipogenic gene expression in liver of aged TAK1$^{-/-}$ mice. *A*: Comparison of cholesterol (Chol), triglyceride (TG), and glucose (levels in liver and serum from 1-year-old WT and TAK1$^{-/-}$ male mice on a normal diet (WT, $n = 6$; TAK1$^{-/-}$, $n = 10$). *B*: Relative food intake by WT and TAK1$^{-/-}$ mice. *C*: Several genes with roles in lipid accumulation are expressed at significantly lower levels in livers of 1-year-old male TAK1$^{-/-}$ mice than those of littermate WT mice (WT, $n = 6$; TAK1$^{-/-}$, $n = 10$). The level of expression was examined by QRT-PCR. Data represent mean ± SEM. *$P < 0.05$; **$P < 0.01$; ***$P < 0.001$.

RESULTS

Generation of TAK1$^{-/-}$ mice. To obtain further insights into the role of TAK1 in vivo, we generated TAK1$^{-/-}$ mutant mice in which TAK1 was functionally inactive (supplementary Fig. 1). Increased mortality of TAK1$^{-/-}$ embryos was noted (supplementary Table 2). Although at 2 to 3 months the surviving TAK1$^{-/-}$ mice were slightly underweight, they were healthy and had a normal appearance and life span. Analysis of multiple organ tissues did not identify any gross anatomical or histologic abnormalities in TAK1$^{-/-}$ mice.

TAK1$^{-/-}$ mice are resistant to age-induced hepatic steatosis. TAK1 is highly expressed in several tissues that are critical in lipid and energy homeostasis (supplementary Fig. 2). To study the role of TAK1 in lipid homeostasis, we first examined whether loss of TAK1 function has any effect on age-induced hepatic steatosis. As shown in Fig. 1*A*, in contrast to aged male WT mice (24), 1-year-old male TAK1$^{-/-}$ mice were protected against age-induced hepatic steatosis (Fig. 1*A*). Heterozygous male TAK1$^{+/-}$ mice developed steatosis to a similar degree as WT littermates (data not shown).

One-year-old male TAK1$^{-/-}$ mice weighed ~30% less (Fig. 1*B*) and the size of epididymal and abdominal WAT, when measured as percentage of total body weight, was markedly reduced (respectively, 50 and 70% less than in WT littermates) (Fig. 1*C*). Histochemical analysis showed reduced lipid accumulation in WAT and BAT of TAK1$^{-/-}$ mice (Fig. 1*A*). Furthermore, adipocytes in WAT of TAK1$^{-/-}$ mice were dramatically smaller than those of WT mice (Fig. 1*D*), suggesting that the reduced adiposity observed in TAK1$^{-/-}$ mice may be caused, to a large extent, by reduced triglyceride accumulation.

Consistent with our histologic observations, biochemical analysis showed that the triglyceride level was greatly reduced in the liver of TAK1$^{-/-}$ mice compared with those of WT mice (Fig. 2*A*). Levels of hepatic cholesterol were slightly, but not significantly, decreased in TAK1$^{-/-}$ mice. Blood triglyceride and cholesterol levels were significantly lower in TAK1$^{-/-}$ mice compared with WT, whereas there was no change in blood glucose levels (Fig. 2*A*). Examination of the food intake over a 5-day period indicated that TAK1$^{-/-}$ mice displayed a modest but significant increased food intake relative to WT mice, suggesting that the reduced fat mass in these mice was not due to reduced food intake (Fig. 2*B*).

Gene expression profiling. To understand the mechanism by which loss of TAK1 prevented age-induced hepatic steatosis, we analyzed and compared the gene expression profiles in liver from WT and TAK1$^{-/-}$ mice by microarray analysis (http://www.ncbi.nlm.nih.gov/geo; accession number GSE21903). Loss of TAK1 function af-

TABLE 1
A partial list of genes up- or downregulated in the liver of 1-year-old TAK1$^{-/-}$ mice compared with WT liver

Functional category	Gene symbol	GenBank accession #	Gene description	Fold change
Metabolism				
Lipid	*Acsm2*	NM_146197	Acyl-CoA synthetase medium-chain family member 2	3.9
	Mgll	NM_011844	Monoglyceride lipase	−1.4
	Dhrs8	NM_053262	Hydroxysteroid (17-β) dehydrogenase 11	−1.5
	Adfp	NM_007408	Adipose differentiation related protein	−1.5
	Adipor2	NM_197985	Adiponectin receptor 2	−1.5
	Lrp4	NM_172668	Low-density lipoprotein receptor-related protein 4	−1.6
	Acox1	NM_015729	Acyl-coenzyme A oxidase 1, palmitoyl	−1.7
	Lpin1	NM_015763	Lipin 1/fatty liver dystrophy protein	−1.8
	Ehhadh	NM_023737	Enoyl-Co A, hydratase/3-hydroxyacyl Co A dehydrogenase	−1.8
	Acaa1b	NM_146230	Acetyl-coenzyme A acyltransferase 1B	−1.8
	Acad10	NM_028037	Acyl-CoA dehydrogenase family member 10	−1.8
	Dgat2l4	NM_177746	Acyl-CoA wax alcohol acyltransferase 2	−1.8
	Fabp2	NM_007980	Fatty acid-binding protein 2, intestinal	−1.8
	Acaa1a	NM_130864	Acetyl-coenzyme A acyltransferase 1A	−1.9
	Crat	NM_007760	carnitine acetyltransferase	−2.0
	Acss2	AK035497	Acyl-CoA synthetase short-chain family member 2	−2.1
	Elovl5	NM_134255	ELOVL family member 5, elongation of long chain fatty acids	−2.2
	Acot2	NM_134188	Acyl-CoA thioesterase 2	−2.2
	Gpam	NM_008149	Glycerol-3-phosphate acyltransferase, mitochondrial	−2.6
	Acot11	NM_025590	Acyl-CoA thioesterase 11	−3.9
	Cd36	NM_007643	CD36 antigen	−3.9
	Mogat1	NM_026713	Monoacylglycerol O-acyltransferase 1	−14.6
	Cidec	NM_178373	Cell death-inducing DFFA-like effector c (FSP27)	−18.0
	Cidea	NM_007702	Cell death-inducing DFFA-like effector A	−94.3
Carbohydrate	*Car2*	NM_009801	Carbonic anhydrase 2	−1.6
Steroid	*Osbpl3*	AK040984	Oxysterol binding protein-like 3	−4.2
Glutathione	*Mgst3*	NM_025569	Microsomal glutathione S-transferase 3	−1.5
	Gstt1	NM_008185	Glutathione S-transferase, theta 1	−1.6
	Gstt2	NM_010361	Glutathione S-transferase, theta 2	−1.7
	Gstt3	NM_133994	Glutathione S-transferase, theta 3	−2.2
Cytochrome c	*Cox7a1*	NM_009944	Cytochrome c oxidase, subunit VIIa 1	−1.6
Oxidase VIIb	*Cox8b*	NM_007751	Cytochrome c oxidase, subunit VIIIb	−4.4
Cytochrome P450	*Cyp2c70*	NM_145499	Cytochrome P450, family 2, subfamily c, polypeptide 70	2.0
	Cyp2c40	NM_010004	Cytochrome P450, family 2, subfamily c, polypeptide 40	2.0
	Cyp39a1	NM_018887	Cytochrome P450, family 39, subfamily a, polypeptide 1	1.8
	Cyp51	NM_020010	Cytochrome P450, family 51	1.7
	Cyb5b	NM_025558	Cytochrome P450, family 5 type B	−1.5
	Cyp2a5	NM_007812	Cytochrome P450, family 2, subfamily a, polypeptide 5	−1.7
	Cyp2a4	NM_009997	Cytochrome P450, family 2, subfamily a, polypeptide 4	−2.0
	Cyp4a10	NM_010011	Cytochrome P450, family 4, subfamily a, polypeptide 11	−2.7
Others	*Asns*	NM_012055	Asparagine synthetase	26.8
	Arsa	NM_009713	Arylsulfatase A	−1.6
	Aldh3a2	NM_007437	Aldehyde dehydrogenase family 3, subfamily A2	−1.9
	Uck1	NM_011675	Uridine-cytidine kinase 1	−2.0
	Wwox	NM_019573	WW domain-containing oxidoreductase	−2.0
	Rdh16	NM_009040	Retinol dehydrogenase 16	−2.3
Transcription	*Onecut1*	BC023444	One cut domain, family member 1 (Hnf6)	3.0
	Foxa1	NM_008259	Forkhead box A1 (Hnf3a)	2.0
	Srebf2	AF374267	Sterol regulatory element binding factor 2	1.4
	Rxrg	NM_009107	Retinoid X receptor γ	−1.4
	Ppargc1b	NM_133249	Peroxisome proliferative activated receptor, γ, coactivator 1 β	−1.5
	Ar	NM_013476	Androgen receptor	−1.5
	Nfe2l2	AK029360	Nuclear factor, erythroid derived 2, like 2	−1.6
	Pparg	NM_011146	Peroxisome proliferator activated receptor γ	−1.9
	Srebf1	NM_011480	Sterol regulatory element binding transcription factor 1	−2.1
Transport	*Apom*	NM_018816	Apolipoprotein M	2.0
	Abcb9	NM_019875	ATP-binding cassette, subfamily B (MDR/TAP), member 9	−1.7
	Abcb1a	NM_011076	ATP-binding cassette, subfamily B (MDR/TAP), member 1A	−2.1
	Abcd3	AK031611	ATP-binding cassette, subfamily D (ALD), member 3	−2.3

Continued on facing page

TABLE 1
Continued

Functional category	Gene symbol	GenBank accession #	Gene description	Fold change
Solute carrier	*Slc25a14*	NM_011398	Solute carrier family 25	−1.4
	Slc27a4	NM_011989	Solute carrier family 27 (FATP4)	−1.5
	Slc5a6	NM_177870	Solute carrier family 5	−1.9
	Slc13a4	NM_172892	Solute carrier family 13	−4.2
Growth/differentiation factors	*Fgfr1*	NM_010206	Fibroblast growth factor receptor 1	3.3
	Ctgf	NM_010217	Connective tissue growth factor	2.1
	Bmp7	NM_007557	Bone morphogenetic protein 7	−1.5
	Vegfb	NM_011697	Vascular endothelial growth factor B	−1.6
	Gdf15	NM_011819	Growth differentiation factor 15 (Mic-1)	−2.4
	Fgf9	NM_013518	Fibroblast growth factor 9	−4.1
G-protein coupled receptor protein signaling	*Avpr1a*	NM_016847	Arginine vasopressin receptor 1A	3.6
	Adra1a	NM_013461	Adrenergic receptor, α 1a	−2.0
	Gprc5b	NM_022420	G protein-coupled receptor, family C, group 5, member B	−10.9
Sulfotransferase	*Sult1c2*	NM_026935	Sulfotransferase 1C, member 2	−2.3
Immune response	*Tff3*	NM_011575	Trefoil factor 3, intestinal	4.2
	Tlr5	NM_016928	Toll-like receptor 5	−1.8
	Cxcl7	NM_023785	Chemokine (C-X-C motif) ligand 7	−2.2
	Raet1a	NM_009016	Retinoic acid early transcript 1, alpha	−3.0
Miscellaneous	*Sqle*	NM_009270	Squalene epoxidase	2.6
	Fbln2	NM_007992	Fibulin 2	2.6
	Inhba	NM_008380	Inhibin β-A	2.0
	Fbxo7	AK082146	F-box protein 7	−1.9
	Insl6	NM_013754	Insulin-like 6	−2.5
	Adam11	BC054536	a disintegrin and metallopeptidase domain 11	−3.6
	Retn	NM_022984	Resistin	−3.7
	Dyx1c1	NM_026314	Dyslexia susceptibility 1 candidate 1 homolog	−11.6

Note: Of the 40,000 transcripts analyzed, the expression of 490 transcripts was decreased by ≥1.5-fold, whereas the expression of 260 transcripts was enhanced by ≥1.5-fold in livers of TAK1$^{-/-}$ mice compared with WT mice.

fected the expression of many genes that are implicated in lipid, fatty acid, and carbohydrate metabolism (Table 1). Cell death-inducing DFFA-like effector c (Cidec), also termed fat-specific protein (FSP27), and cell death-inducing DFFA-like effector a (Cidea), two proteins that play a critical role in triglyceride accumulation (25–27), monoacylglycerol O-acyltransferase one (Mogat1), which is part of an alternative pathway of triglyceride synthesis, and CD36, which plays a role in lipid transport and steatosis (28), were among the genes most strongly suppressed in TAK1$^{-/-}$ liver. Thus, these observations suggest that TAK1 positively regulates the expression of several genes encoding proteins involved in promoting lipid uptake and triglyceride accumulation.

Among other notable changes, the expression of a number of phase I and phase II enzyme, and drug-transporter genes was affected in TAK1$^{-/-}$ livers, including several cytochrome p450 enzymes, sulfotransferase Sult1c2, and several ATP-binding cassette (Abc) transporters (Table 1). These observations suggest that TAK1 may also play a role in the regulation of the transport and metabolism of various drugs and xenobiotics. Several transcription factors, including Srebf1 and Pparγ, were expressed at significantly lower levels in TAK1$^{-/-}$ liver compared with WT liver, whereas Onecut1 and Foxa1 were expressed at higher levels in the liver of TAK1$^{-/-}$ mice.

The repression of hepatic expression of Cidea, Cidec, Gprc5b, Mogat1, resistin (Retn), CD36, Srebf1, acetyl-CoA carboxylase a, and fatty acid binding protein-2 (Fabp2), in TAK1$^{-/-}$ mice was confirmed by QRT-PCR (Fig. 2*C*). The expression of the corepressor RIP140, which has been reported to regulate Cidea (29), was not significantly different between TAK1$^{-/-}$ and WT mice. The repression of Pparγ in TAK1$^{-/-}$ liver was confirmed by QRT-PCR, whereas the expressions of estrogen-related receptor α (ERRα), pregnane X receptor (PXR), and liver X receptor α (LXRα) were not changed in the liver of TAK1$^{-/-}$ mice (Fig. 2*C*).

We next examined whether the changes in gene expression in aged mice could be detected at an earlier age. Although histologically no significant differences were observed between the livers of 4- to 5-month-old WT and TAK1$^{-/-}$ mice (Fig. 3*A* and *B*), the expression of Cidea, Cidec, Mogat1, Cd36, and Retn was significantly reduced in TAK1$^{-/-}$ liver compared with WT liver (Fig. 3*C*). Moreover, analysis of gene expression in primary hepatocytes showed that Cidea, Cidec, Pparγ, Cd36, and Mogat1 were expressed at significantly lower levels in TAK1$^{-/-}$ primary hepatocytes than in WT hepatocytes (Fig. 3*D*). Next, we examined, whether the expression of genes downregulated in TAK1$^{-/-}$ hepatocytes could be restored by exogenous TAK1 expression. Infection of TAK1$^{-/-}$ hepatocytes with Ad-TAK1 adenovirus restored TAK1 expression and induced Cidea and Mogat1 expression several fold and that of Cidec by 70%, whereas infection with Ad-Empty or Ad-TAK1ΔAF2, in which the activation domain of TAK1 was deleted, had little effect on the expression of these genes (Fig. 3*E*). Expression of Pparγ was not significantly altered by Ad-TAK1, suggesting that the increase in Cidea, Cidec, and Mogat1 mRNA occurred independently of the increased Pparγ mRNA expression.

TAK1$^{-/-}$ mice are resistant to HFD-induced hepatic steatosis. TAK1$^{-/-}$ mice were also protected against HFD-induced hepatic steatosis and obesity. The 8- to 10-week-old TAK1$^{-/-}$ mice fed a HFD for 6 weeks gained

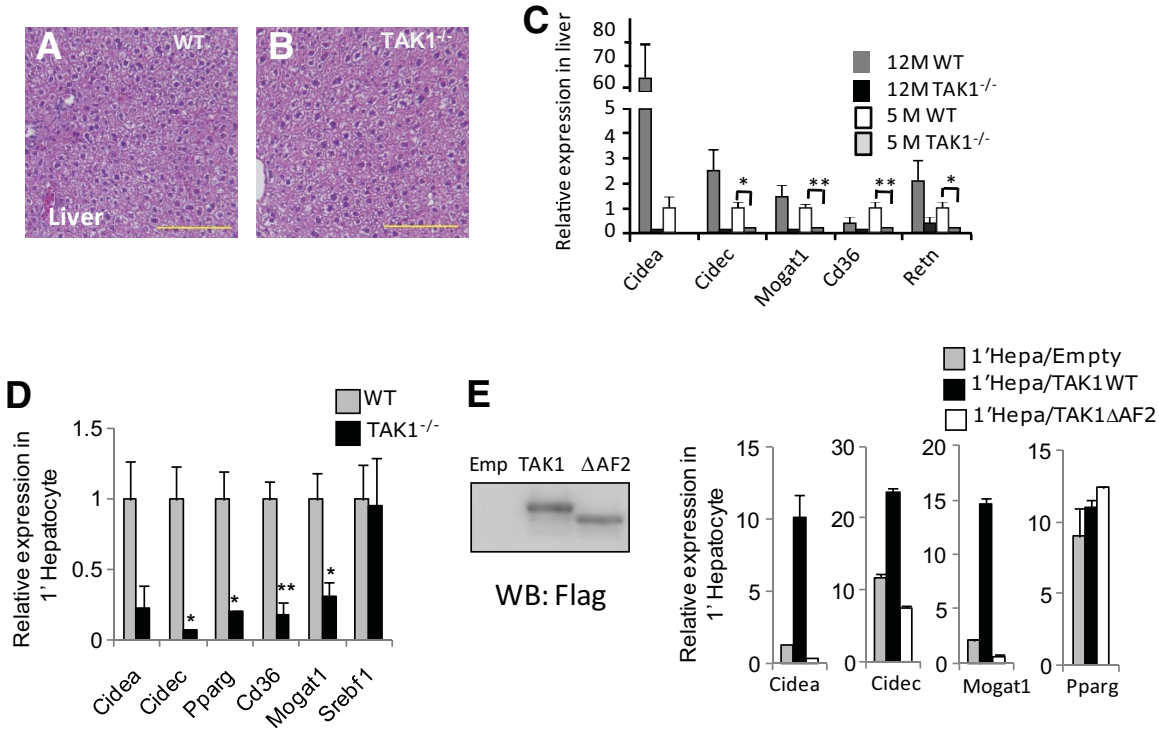

FIG. 3. Changes in lipogenic gene expression in liver and primary hepatocytes from 4- to 5-month-old, chow-fed TAK1$^{-/-}$ mice. *A* and *B*: Representative H&E-stained sections of liver from WT and TAK1$^{-/-}$ male mice. Scale bar indicates 200 μm. *C*: Reduced expression of several lipogenic genes in liver of 4- to 5-month-old male TAK1$^{-/-}$ mice compared with WT littermates (WT, $n = 5$; TAK1$^{-/-}$, $n = 4$). Hepatic gene expression was also compared between 1-year-old and 4- to 5-month-old WT and TAK1$^{-/-}$ mice. Data represent mean ± SEM. *$P < 0.05$; **$P < 0.01$. *D*: Comparison of gene expression between primary hepatocytes from 4- to 5-month-old TAK1$^{-/-}$ and WT mice. *E*: TAK1$^{-/-}$ hepatocytes were infected with Ad-Empty, Ad-TAK1WT, or Ad-TAK1ΔAF2 adenovirus, and 72 h later analyzed for Cidea, Mogat1, Cidec, and Pparγ expression by QRT-PCR (*right panel*). The expression of TAK1 and TAK1ΔAF2 was confirmed by Western blot using anti-Flag M2 antibody (*left panel*). (A high-quality color representation of this figure is available in the online issue.)

less weight than their WT littermates (Fig. 4*A*). By the end of the feeding period, the average body weight of WT mice increased by 55%, whereas TAK1$^{-/-}$ mice gained only 12% body weight. TAK1$^{-/-}$(HFD) mice also exhibited a reduced fat mass compared with WT(HFD) controls. In fact, the relative weight of epididymal and abdominal WAT in TAK1$^{-/-}$(HFD) mice was, respectively, 40 and 50% less compared with WT(HFD) mice, whereas no

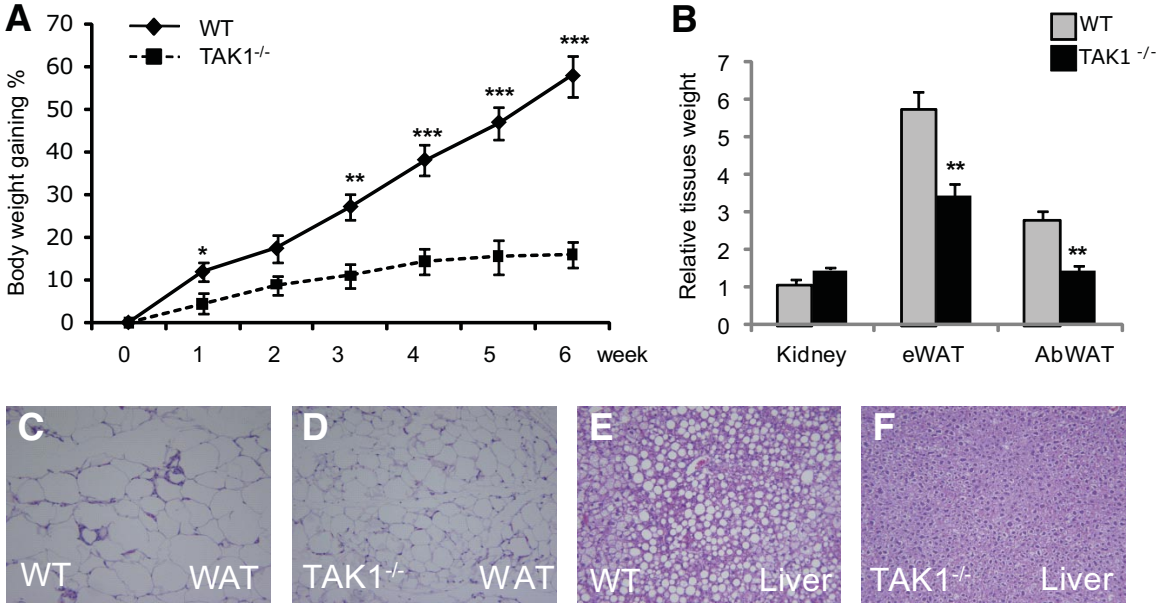

FIG. 4. TAK1$^{-/-}$ mice are resistant to diet-induced obesity. Ten-week-old male mice were fed a HFD for 6 weeks. *A*: The percentage of body weight gain was calculated based on the body weight at the start of the HFD. The average body-weight gains of WT ($n = 6$) and TAK1$^{-/-}$ ($n = 6$) mice were calculated and plotted. (*$P < 0.05$; **$P < 0.01$; ***$P < 0.001$). *B*: Comparison of the relative weights of kidneys, eWAT, and AbWAT were determined after 6 weeks on a HFD. *$P < 0.01$. *C–F*: Representative H&E-stained sections of liver and WAT from WT(HFD) and TAK1$^{-/-}$(HFD) mice. (A high-quality color representation of this figure is available in the online issue.)

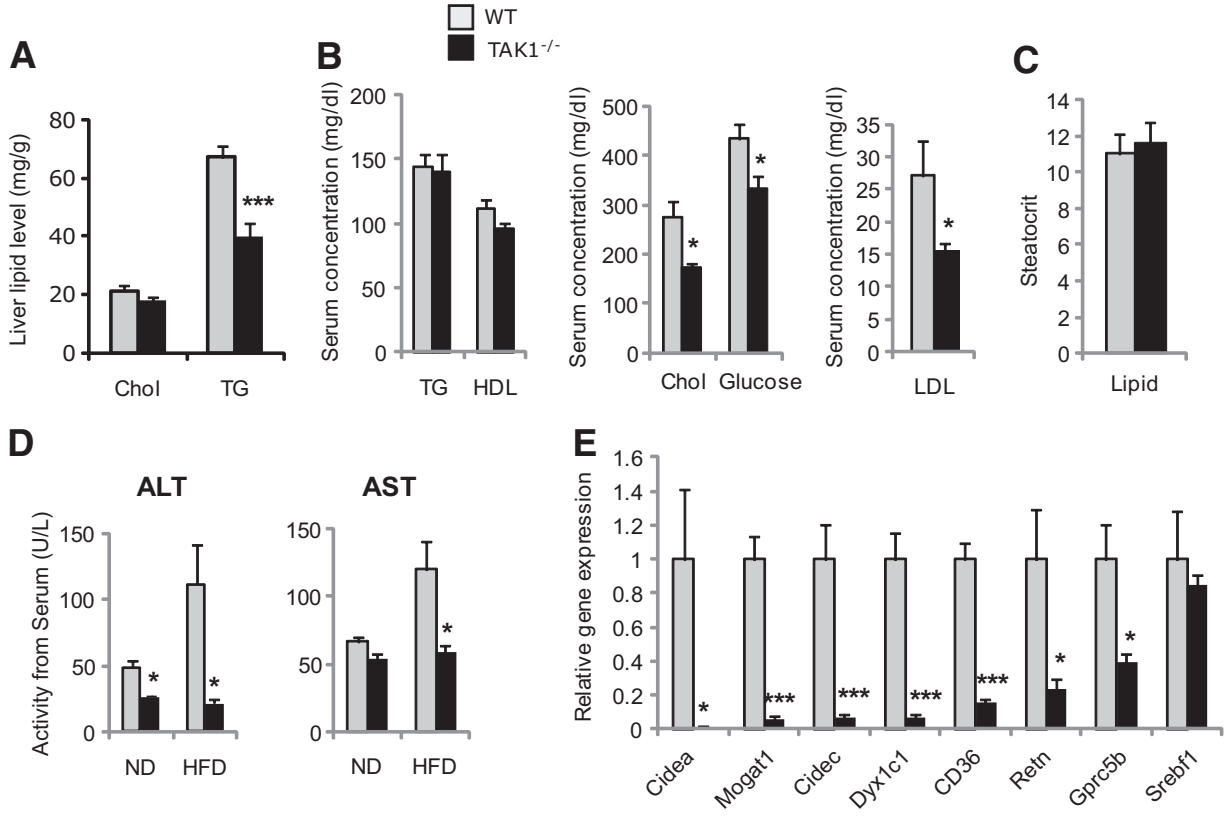

FIG. 5. Reduced lipid accumulation and lipogenic gene expression in liver of TAK1$^{-/-}$ mice fed a HFD. *A*: Comparison of hepatic triglyceride and cholesterol levels in WT(HFD) and TAK1$^{-/-}$(HFD) mice (n = 6) fed a HFD for 6 weeks. *B*: Lipid and glucose levels in serum of WT(HFD) and TAK1$^{-/-}$(HFD) mice. *C*: Steatocrit was analyzed from feces of WT(HFD) and TAK1$^{-/-}$(HFD) mice. *D*: ALT and AST activity in serum of WT(HFD) and TAK1$^{-/-}$(HFD) mice. *E*: Comparison of hepatic gene expression in WT(HFD) and TAK1$^{-/-}$(HFD) mice. Gene expression was analyzed by quantitative RT-PCR. Data represent mean ± SEM. (*P < 0.05; **P < 0.01; ***P < 0.001).

significant difference in kidney weights was observed (Fig. 4*B*).

Histologic analysis revealed that TAK1$^{-/-}$(HFD) mice showed significantly smaller WAT adipocyte size, as well as less accumulation of hepatic lipid droplets than their WT(HFD) littermates (Fig. 4*C*–*F*). The latter was supported by biochemical data showing that the significantly lower hepatic triglyceride accumulation in TAK1$^{-/-}$(HFD) mice than in WT(HFD) mice (Fig. 5*A*). The serum concentrations of triglycerides and HDL were not significantly changed, but total cholesterol, LDL, and glucose levels were significantly reduced in TAK1$^{-/-}$ mice compared with WT mice (Fig. 5*B*). Together, these observations indicate that TAK1$^{-/-}$ mice were significantly protected against HFD-induced obesity and hepatic steatosis. The protective effect cannot be attributed to increased levels of secreted lipid in the feces, because no appreciable difference was found in that regard between WT and TAK1$^{-/-}$ mice (Fig. 5*C*). Analysis of serum alanine aminotransferase (ALT) and aspartate aminotransferase (AST), markers of hepatocytotoxicity, showed that ALT and AST levels were significantly elevated in WT(HFD) mice compared with TAK1$^{-/-}$(HFD) mice (Fig. 5*D*). Hepatic expression of Cidea, Mogat1, Cidec, CD36, and Retn was significantly lower in TAK1$^{-/-}$(HDF) mice than in WT(HFD) mice (Fig. 5*E*), consistent with observations in aged TAK1$^{-/-}$ mice.

TAK1$^{-/-}$ mice have an increased energy expenditure. Although their relative food consumption was higher (Fig. 6*E*), TAK1$^{-/-}$ mice were leaner than WT mice, which suggested that TAK1$^{-/-}$ mice might have an increased energy expenditure. Using indirect calorimetry, oxygen consumption (VO_2) and CO_2 production (VCO_2) rates were measured in TAK1$^{-/-}$(HFD) and WT(HFD) mice over a period of 2 days. In both WT(HFD) and TAK1$^{-/-}$(HFD) mice, VO_2 and VCO_2 were significantly increased during the dark phase compared with the light phase (Fig. 6*A* and *B*). Moreover, TAK1$^{-/-}$(HFD) mice exhibited elevated VO_2 and VCO_2 in both the light and dark phase as compared with WT(HFD) mice, and an increased respiratory exchange ratio (Fig. 6*A*–*C*). These observations are consistent with a higher rate of energy expenditure by TAK1$^{-/-}$(HFD) mice that might be partly caused by the observed increase in heat generation (Fig. 6*D*), The increased expression of uncoupling protein 1 (Ucp1), CoxIV, and Pgc-1α in BAT of TAK1$^{-/-}$(HFD) mice, compared with that of WT(HFD), is consistent with the notion of increased energy expenditure (Fig. 6*F*).

Inflammation was significantly reduced in WAT of TAK1$^{-/-}$(HFD) mice. WAT-associated inflammation plays a critical role in the development of obesity-related complications (6–8,30). Consistent with this, WAT of WT(HFD) mice showed an increase in crown-like structures (CLS) representing aggregated F4/80-positive macrophages (Fig. 7*A*). In contrast, F4/80-positive cells were infrequently observed in WAT from TAK1$^{-/-}$(HFD) mice (Fig. 7*A*). This was substantiated by quantitative analysis showing that the percentage of SVF-associated macrophages (F4/80$^+$/Cd11b$^+$) was significantly reduced in TAK1$^{-/-}$(HFD) mice compared with WT(HFD) (Fig. 7*B*). Furthermore, the percentage of CD3$^+$ T lymphocytes in TAK1$^{-/-}$(HFD) mice was 45% lower than in WT mice;

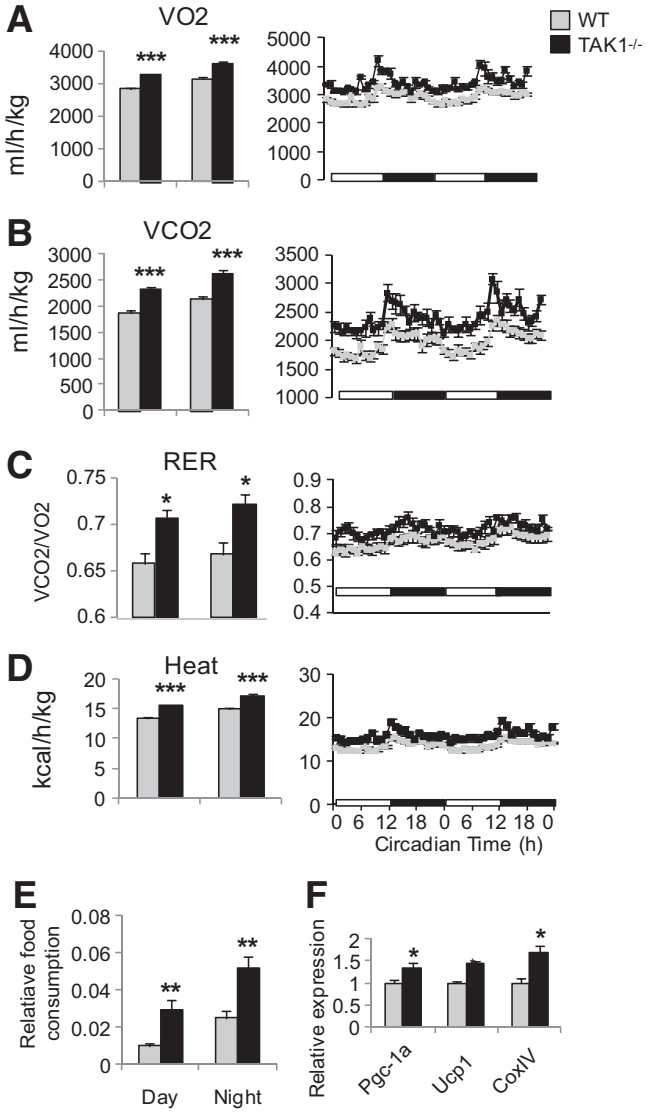

FIG. 6. TAK1$^{-/-}$ mice have increased energy expenditure. *A–D*: Oxygen consumption (VO_2) and carbon dioxide generation (VCO_2) by WT(HFD) and TAK1$^{-/-}$(HFD) were analyzed by indirect calorimetry during two 12-h light/12-h dark cycles (WT, $n = 6$, TAK1$^{-/-}$, $n = 5$). Respiratory exchange ratio (RER) and heat generation were computed. *E*: Relative food consumption of WT and TAK1$^{-/-}$ mice during light and dark periods. *F*: Increased expression of Ucp-1, CoxIV, and Pgc-1α in BAT of TAK1$^{-/-}$(HFD) mice compared with WT(HFD) littermates. Gene expression was analyzed by quantitative RT-PCR. Data represent mean ± SEM. *$P < 0.05$, **$P < 0.01$, ***$P < 0.001$.

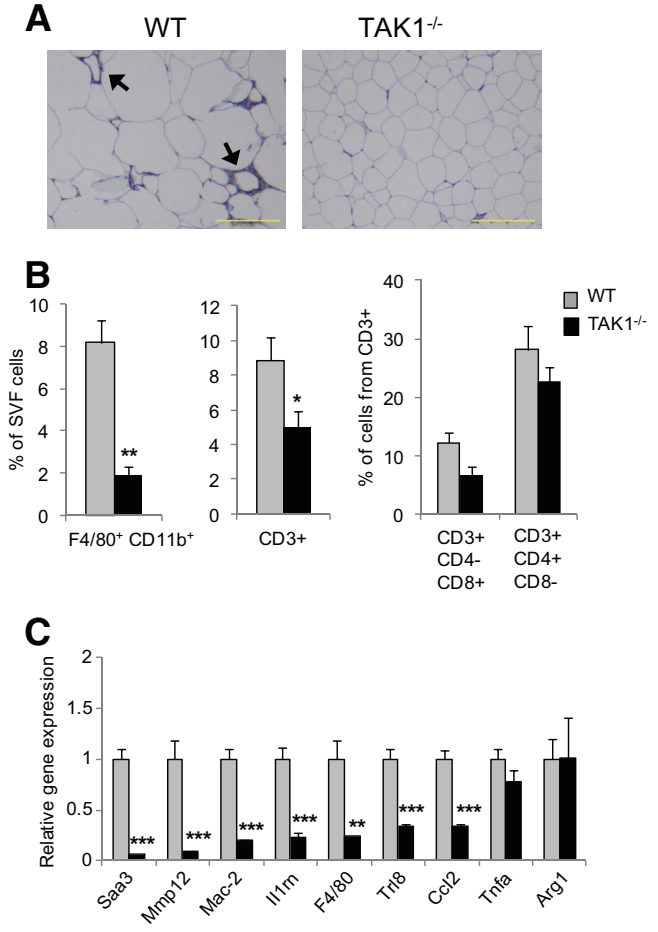

FIG. 7. WAT-associated inflammatory response is reduced in TAK1$^{-/-}$(HFD) mice. *A*: Macrophage infiltration into eWAT was greatly reduced in TAK1$^{-/-}$ mice. F4/80$^+$ macrophages were identified by immunohistochemical staining as "crown-like structures" (*arrows*). Scale bar indicates 250 μm. *B*: SVF cells from eWAT of WT(HFD) and TAK1$^{-/-}$(HFD) mice were examined by fluorescence-activated cell sorter analysis. The percentages of macrophages (F4/80$^+$CD11b$^+$ cells), T lymphocytes (CD3$^+$ cells), and CD8$^+$andCD4$^+$ T cells were determined (WT, $n = 6$; TAK1$^{-/-}$, $n = 4$). Data represent mean ± SEM. *$P < 0.05$. *C*: Induction of inflammatory genes was greatly decreased in WAT of TAK1$^{-/-}$(HFD) mice ($n = 5$) compared with WT mice ($n = 5$). Gene expression was analyzed by quantitative RT-PCR. Data represent mean ± SEM. *$P < 0.05$, **$P < 0.01$, ***$P < 0.001$. (A high-quality color representation of this figure is available in the online issue.)

however, the ratio between CD4$^+$ and CD8$^+$ T cells was not different, indicating that both CD4$^+$ and CD8$^+$ cell populations are decreased in the WAT of TAK1$^{-/-}$(HFD) mice (Fig. 7*B*). Together, these results suggest that loss of TAK1 greatly reduced HFD-responsive inflammation in WAT. The inhibition of inflammation in WAT of TAK1$^{-/-}$(HFD) mice was supported by decreased expression of the macrophage markers, F4/80 and Mac-2, and several other inflammation-related genes, including serum amyloid-3 (*Saa3*), matrix metallopeptidase 12 (*Mmp12*), interleukin-1 receptor antagonist (*Il1rn*), and the Toll-like receptor 8 (*Tlr8*) compared with WT(HFD) WAT (Fig. 7*C*). In addition, as observed in TAK1$^{-/-}$(HFD) mice, the expression of *Mmp12*, *Saa3*, *Mac-2*, and *F4/80* was also significantly reduced in WAT of 1-year-old TAK1$^{-/-}$ mice compared with their age-matched WT mice (supplementary Fig. 3).

These data support the hypothesis that TAK1$^{-/-}$ mice are protected against obesity-associated inflammation of adipose tissue.

TAK1$^{-/-}$ mice are protected against insulin resistance. It is well established that obesity greatly enhances the risk of type 2 diabetes as indicated by the development of insulin resistance and glucose intolerance (3,4). As shown in Fig. 8*A*, blood insulin levels were significantly lower in chow-fed, 4- to 5-month-old TAK1$^{-/-}$ mice compared with their age-matched WT littermates. Insulin levels increased further in aged WT and WT(HFD) mice, but remained low in corresponding TAK1$^{-/-}$ littermates. Moreover, WT(HFD) mice developed glucose intolerance and insulin resistance as indicated by the glucose tolerance test and insulin tolerance test analyses (Fig. 8*B* and *C*). In sharp contrast, TAK1$^{-/-}$(HFD) mice retained their glucose tolerance and insulin sensitivity, indicating that TAK1$^{-/-}$ mice are protected against insulin resistance, a common symptom of diabetes.

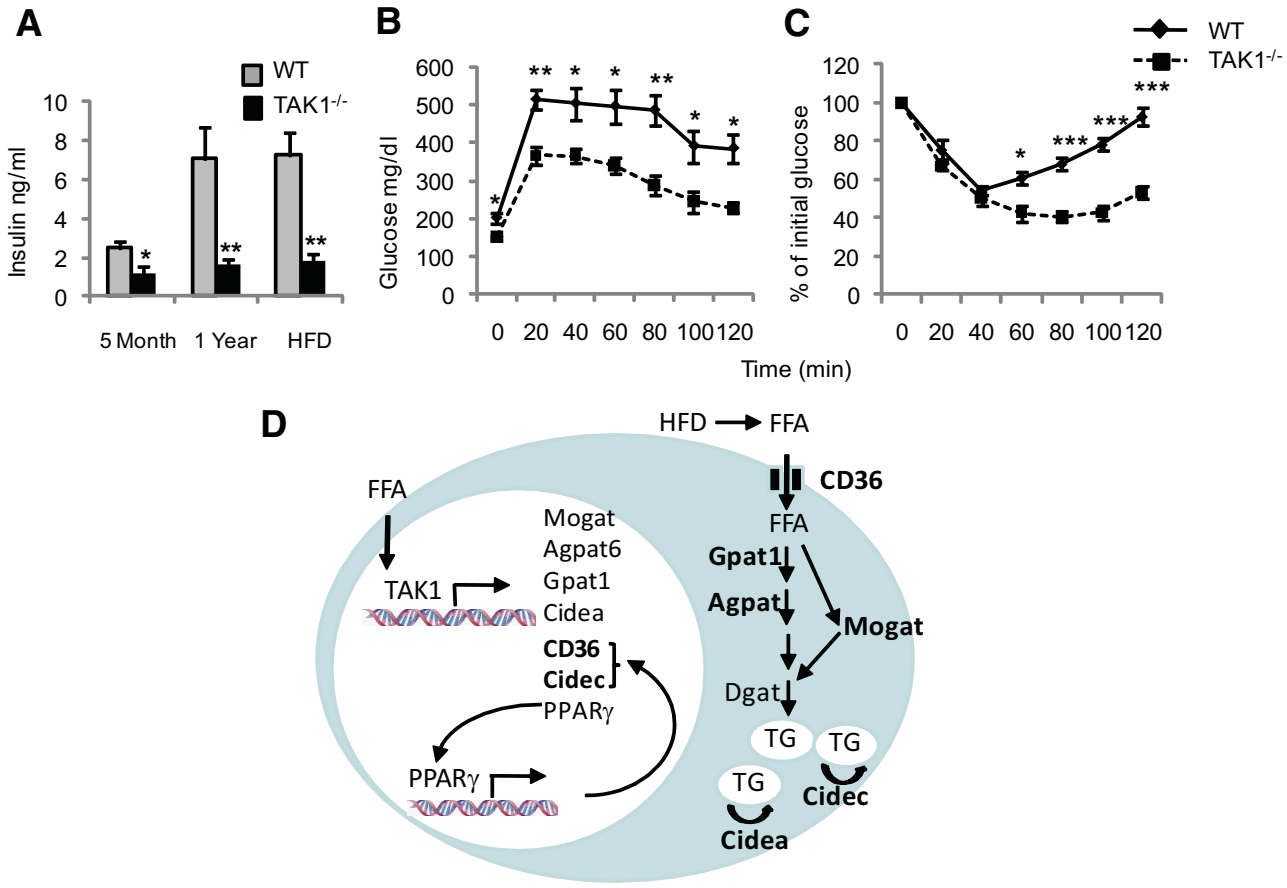

FIG. 8. TAK1$^{-/-}$ mice are protected against HFD-induced insulin resistance and glucose intolerance. *A*: Blood insulin levels were analyzed in 5-month-old mice (WT, $n = 5$; TAK1$^{-/-}$, $n = 4$), 1-year-old mice (WT, $n = 8$; TAK1$^{-/-}$, $n = 9$), and mice fed a HFD (WT, $n = 10$; TAK1$^{-/-}$, $n = 7$). B, *C*: Glucose tolerance test (GTT) and insulin tolerance test (ITT) analyses in WT(HFD) and TAK1$^{-/-}$(HFD) mice (WT, $n = 5$; TAK1$^{-/-}$, $n = 4$). Blood samples were drawn and glucose levels analyzed every 20 min for up to 2–2.5 h. Data represent mean ± SEM. *$P < 0.05$, **$P < 0.01$, ***$P < 0.001$. *D*: Schematic view of the potential role of TAK1/TR4 in lipid homeostasis and hepatic steatosis. Elevated levels of fatty acids during aging and HFD may promote the activation of TAK1 leading to increased transcription of TAK1-responsive genes, such as *CD36*, *Cidec*, *Cidea*, and *Mogat1*. The induction of these proteins then lead to increased fatty acid uptake and triglyceride synthesis and storage, and promote hepatic steatosis. Induced expression of other transcription factors, such as PPARγ, by TAK1 can also lead to the activation of *CD36*, *Cidec*, or other lipogenic genes and may provide an alternative way to further enhance hepatic triglyceride accumulation. (A high-quality color representation of this figure is available in the online issue.)

DISCUSSION

In this study we show, for the first time, that loss of TAK1 protects mice against age- and HFD-induced metabolic syndrome. TAK1$^{-/-}$ mice remain lean and show reduced adiposity and hepatic steatosis during aging or when fed a HFD. Moreover, TAK1$^{-/-}$ mice are protected against the development of age- and diet-induced adipose tissue-associated inflammation, insulin resistance, and glucose intolerance. These observations indicate that the nuclear receptor TAK1 plays a critical role in the control of energy balance and lipid homeostasis.

Livers of TAK1$^{-/-}$ mice showed a reduced lipid accumulation compared with their WT littermates. Hepatic triglyceride accumulation is controlled at several levels, including fatty acid uptake, synthesis and storage of triglycerides, fatty acid oxidation, and lipolysis. Gene expression profiling revealed a great number of differences in gene expression between livers from 1-year-old WT and TAK1$^{-/-}$ mice, including genes that are critical in the regulation of lipid, fatty acid, carbohydrate, and xenobiotic metabolism, and gene transcription (Table 1). The expression of many of these genes has been reported to be elevated in hepatic steatosis (31,32). One of these genes is CD36, which encodes a multifunctional protein implicated in angiogenesis, immunity, and in several metabolic disorders, such as obesity, hepatic steatosis, and insulin resistance (28,33). In several cell types, including adipocytes and hepatocytes, CD36 facilitates long-chain fatty acid uptake. Thus, the reduced CD36 expression observed in TAK1$^{-/-}$ liver may lead to diminished hepatic fatty acid uptake and, at least in part, be responsible for the resistance to hepatic steatosis.

Cidea and Cidec were also among the genes that were the most dramatically downregulated in TAK1$^{-/-}$ mice. Cide proteins promote triglyceride accumulation within lipid droplets and regulate lipolysis, and their expression correlates positively with the development of obesity and hepatic steatosis (25,34,35). Deficiency in Cidea or Cidec in mice resulted in increased energy expenditure and lipolysis, and yielded a lean phenotype in mice and resistance to diet-induced obesity (25,26,36). Therefore, the repression of these genes in TAK1$^{-/-}$ mice may also have contributed to the reduction in hepatic triglyceride levels and resistance to hepatic steatosis in TAK1$^{-/-}$ mice. Although the expression of Cidea and Cidec, as well as CD36, was greatly repressed in the liver of TAK1$^{-/-}$ mice, TAK1 did not appear to regulate the expression of these genes in WAT, suggesting a tissue-dependent regulation.

Mogat1, another gene that was dramatically downregulated in TAK1$^{-/-}$ liver, is part of an alternative, less-studied pathway of triglyceride synthesis. The main pathway of triglyceride synthesis is catalyzed by glycerol-3-phosphate acyltransferase (GPAT), acyl-glycerol-3-phosphate acyltransferases (AGPATs), and diacylglycerol transferase (DGAT) in the final step of synthesis (37). The expression of DGAT1 was not altered; however, the expression of GPAT1 and AGPAT6 was significantly reduced in TAK1$^{-/-}$ liver. The latter is interesting because AGPAT6-deficiency has been reported to cause lipodystrophy and resistance to obesity (38). Thus, the lower levels of Mogat1, GPAT1, and AGPAT6 expression may be part of the mechanism by which triglyceride synthesis and storage is reduced in TAK1$^{-/-}$ liver. Thus, the regulation of several genes with functions related to fatty acid uptake (*CD36*), triglyceride synthesis (*Mogat1*, *GPAT1*, *AGPAT6*), and storage (*Cidea*, *Cidec*) suggests that TAK1 affects several aspects of lipid accumulation. In contrast, no significant changes in fatty acid oxidation were observed.

In contrast to aged mice, 4- to 5-month-old mice fed with a normal diet did not show histologic signs of hepatic steatosis; however, the hepatic expression of Cidea, Cidec, Mogat1, CD36, and Retn was significantly lower in TAK1$^{-/-}$ mice than WT littermates. Consistent with a previous study (19), young TAK1 KO mice were also more glucose tolerant and insulin sensitive than WT mice (supplementary Fig. 4). These observations suggest that TAK1 affects changes in hepatic gene expression and insulin sensitivity at an early age.

Energy and lipid homeostasis is under the control of a complex network of transcription factors and coregulators (32,39–41). Deficiencies in many of these factors have been associated with resistance to diet-induced obesity. For example, mice deficient in the nuclear receptors COUP-TFII and ERRα, or the coregulator RIP140 exhibit a lean phenotype; however, the expression of these genes was unaltered in TAK1$^{-/-}$ liver. Because TAK1 itself functions as a transcription factor, one might expect that some of the differentially expressed genes be regulated directly by TAK1. Indeed, a recent report showed that TAK1 regulates *CD36* transcription in macrophages by binding to TAK1 response elements in the *CD36* gene promoter (14), suggesting that *CD36* is a direct TAK1 target gene. *CD36* is also a known target of several other nuclear receptors, including PPARγ, LXR, and PXR (42). Although the expression of PXR and LXR was unchanged, the expression of PPARγ was reduced by 50% in liver of TAK1$^{-/-}$ mice. Therefore, hepatic CD36 expression might be regulated by TAK1 directly as well as indirectly through modulation of PPARγ expression (Fig. 8*D*). The coregulators RIP140 and PGC-1α, and the receptor PPARγ have also been implicated in the regulation of Cidec (29,42,43). TAK1 might cooperate with these transcriptional modulators to regulate the expression of these genes. Moreover, the downregulation of the transcription factor Srebf1, which promotes triglyceride synthesis (44), may contribute to the reduced lipid accumulation in TAK1$^{-/-}$ liver.

Our data also demonstrated that the expression of several lipogenic genes was dramatically decreased in TAK1$^{-/-}$ primary hepatocytes compared with WT hepatocytes. Restoration of TAK1 expression in TAK1$^{-/-}$ hepatocytes by Ad-TAK1 induced the expression of Mogat1, Cidea, and Cidec, whereas empty virus or expression of an inactive form of TAK1 had little effect on their expression level. Moreover, downregulation of TAK1 in Hepa1–6 cells by TAK1 siRNAs suppressed Cidec, whereas stable expression of TAK1-induced Cidec expression. These data indicate that these changes in gene regulation by TAK1 are hepatocyte cell autonomous and not a response to changes in other tissues. Whether these TAK1-responsive genes are direct targets of TAK1 transcriptional regulation needs further study.

Recent studies have provided evidence indicating that TAK1 functions as a ligand-dependent transcription factor. Certain fatty acids, including γ-linoleic acid and γ-linolenic acid, as well as several eicosanoids, have been shown to activate TAK1-mediated transcription, suggesting that TAK1 might function as a fatty acid sensor (13,14). Consistent with this hypothesis, we speculate that during aging or when fed a HFD, elevated levels of fatty acids may result in increased activation of TAK1 and enhanced expression of TAK1-responsive genes, such as CD36, that promote fatty acid uptake and triglyceride accumulation, and subsequent obesity (Fig. 8*D*). Hence, one could speculate that TAK1-selective antagonists would inhibit the expression of these genes and might be useful for the management of metabolic syndrome.

In addition to hepatic steatosis, adiposity is greatly reduced in aged TAK1$^{-/-}$ and TAK1$^{-/-}$(HFD) mice compared with WT mice. The adipocytes in TAK1$^{-/-}$ mice were significantly smaller than in WT mice, suggesting reduced storage of triglycerides. Obesity is well known to be associated with chronic, low-grade inflammation, and there is considerable evidence that inflammation, insulin resistance, and aberrant lipid metabolism are interlinked in metabolic syndrome (3–5,9). Hypertrophy of adipose tissues and infiltration of inflammatory cells have been recognized as important early events in the development of obesity-linked pathologies. The molecular process of the recruitment and function of macrophage infiltration is not fully understood; however, the release of various cytokines by adipose tissue is likely part of the recruitment of various immune cells (6–8). In contrast to WT mice, TAK1$^{-/-}$ mice are protected against the development of age- and diet-induced adipose tissue-associated inflammation, as indicated by reduced infiltration of macrophages and T lymphocytes. Crown-like structures were rarely observed in WAT of TAK1$^{-/-}$ mice and the macrophage markers, F4/80 and Mac-2, were expressed at significantly lower levels. In addition, the expression of several proinflammatory genes, including *Saa3*, *Mmp-12*, *Il1rn*, and *Tlr8*, were also reduced in adipose tissues of TAK1$^{-/-}$ mice. T lymphocytes have also been implicated in the development of obesity-associated complications (6–8,30). CD8^{+} effector T cells have been reported to exhibit an essential role in the initiation and maintenance of adipose tissue inflammation, including macrophage recruitment, during obesity. The observed reduction in the number of CD8^{+} cells in SVF might be linked to the diminished infiltration of macrophages and inflammatory response in TAK1$^{-/-}$ mice. Moreover, the reduced WAT inflammation in TAK1$^{-/-}$ mice may in part be responsible for the preservation of the insulin sensitivity and glucose tolerance observed in TAK1$^{-/-}$ mice. In this regard, the repression of Il1rn expression in TAK1$^{-/-}$ WAT is particularly interesting because upregulation of this gene has been reported to be associated with obesity whereas Il1rn KO mice have been shown to be resistant to obesity (45,46). Therefore, repression of this gene may contribute to the resistance to obesity observed in TAK1 KO mice.

Finally, two important factors in energy balance are

food intake and energy expenditure. Although their relative food intake was slightly higher than their WT littermates, TAK1$^{-/-}$ mice exhibited a lean phenotype compared with WT mice. Furthermore, TAK1$^{-/-}$ mice showed a significant increase in energy expenditure as indicated by increased oxygen consumption and CO_2 production rates. The increase in energy expenditure by TAK1$^{-/-}$ mice is consistent with the elevated expression of UCP1 in BAT. UCP1 diverts energy derived from mitochondrial electron transport chain and generation of ATP into heat production. Thus, the elevated energy expenditure observed in TAK1$^{-/-}$(HFD) mice may at least in part be responsible for the reduced weight gain and resistance to hepatic steatosis and insulin insensitivity.

In summary, in this study we show for the first time that TAK1$^{-/-}$ mice are protected against age- and HFD-induced obesity, hepatic steatosis, adipose tissue-associated inflammation, and insulin resistance. As a ligand-dependent nuclear receptor, TAK1 might provide a novel therapeutic target in the management and prevention of obesity and related pathologies, such as diabetes.

ACKNOWLEDGMENTS

This research was supported by the Intramural Research Program of the National Institute of Environmental Health Sciences (NIEHS), National Institutes of Health (Z01-ES-101586).

No potential conflicts of interest relevant to this article were reported.

H.S.K. researched data and wrote the manuscript. K.O., Y.T., H.D., T.W., X.-P.Y., and G.L. researched data. Y.-S.K., C.D.B., and W.X. researched data and reviewed/edited the manuscript. A.M.J. wrote the manuscript.

The authors thank Drs. Kristin Lichti-Kaiser, Gary Zeruth, and Xiaoling Li, NIEHS, for their valuable comments on the manuscript; Laura Miller, NIEHS, for her assistance with the mice; and Dr. Kevin Gerrish of the NIEHS Microarray Group for assistance with the microarray analysis.

REFERENCES

1. Browning JD, Szczepaniak LS, Dobbins R, Nuremberg P, Horton JD, Cohen JC, Grundy SM, Hobbs HH. Prevalence of hepatic steatosis in an urban population in the United States: impact of ethnicity. Hepatology 2004;40:1387–1395
2. Ogden CL, Flegal KM, Carroll MD, Johnson CL. Prevalence and trends in overweight among US children and adolescents, 1999–2000. JAMA 2002;288:1728–1732
3. Hotamisligil GS. Inflammation and metabolic disorders. Nature 2006;444:860–867
4. Schenk S, Saberi M, Olefsky JM. Insulin sensitivity: modulation by nutrients and inflammation. J Clin Invest 2008;118:2992–3002
5. Tilg H, Moschen AR. Adipocytokines: mediators linking adipose tissue, inflammation and immunity. Nat Rev Immunol 2006;6:772–783
6. Nishimura S, Manabe I, Nagasaki M, Eto K, Yamashita H, Ohsugi M, Otsu M, Hara K, Ueki K, Sugiura S, Yoshimura K, Kadowaki T, Nagai R. CD8+ effector T cells contribute to macrophage recruitment and adipose tissue inflammation in obesity. Nat Med 2009;15:914–920
7. Weisberg SP, McCann D, Desai M, Rosenbaum M, Leibel RL, Ferrante AW Jr. Obesity is associated with macrophage accumulation in adipose tissue. J Clin Invest 2003;112:1796–1808
8. Feuerer M, Herrero L, Cipolletta D, Naaz A, Wong J, Nayer A, Lee J, Goldfine AB, Benoist C, Shoelson S, Mathis D. Lean, but not obese, fat is enriched for a unique population of regulatory T cells that affect metabolic parameters. Nat Med 2009;15:930–939
9. Odegaard JI, Chawla A. Mechanisms of macrophage activation in obesity-induced insulin resistance. Nat Clin Pract Endocrinol Metab 2008;4:619–626
10. Chang C, Da Silva SL, Ideta R, Lee Y, Yeh S, Burbach JP. Human and rat TR4 orphan receptors specify a subclass of the steroid receptor superfamily. Proc Natl Acad Sci U S A 1994;91:6040–6044
11. Chang C, Kokontis J, Acakpo-Satchivi L, Liao S, Takeda H, Chang Y. Molecular cloning of new human TR2 receptors: a class of steroid receptor with multiple ligand-binding domains. Biochem Biophys Res Commun 1989;165:735–741
12. Hirose T, Fujimoto W, Tamaai T, Kim KH, Matsuura H, Jetten AM. TAK1: molecular cloning and characterization of a new member of the nuclear receptor superfamily. Mol Endocrinol 1994;8:1667–1680
13. Tsai NP, Huq M, Gupta P, Yamamoto K, Kagechika H, Wei LN. Activation of testicular orphan receptor 4 by fatty acids. Biochim Biophys Acta 2009;1789:734–740
14. Xie S, Lee YF, Kim E, Chen LM, Ni J, Fang LY, Liu S, Lin SJ, Abe J, Berk B, Ho FM, Chang C. TR4 nuclear receptor functions as a fatty acid sensor to modulate CD36 expression and foam cell formation. Proc Natl Acad Sci U S A 2009;106:13353–13358
15. Chen YT, Collins LL, Uno H, Chang C. Deficits in motor coordination with aberrant cerebellar development in mice lacking testicular orphan nuclear receptor 4. Mol Cell Biol 2005;25:2722–2732
16. Collins LL, Lee YF, Heinlein CA, Liu NC, Chen YT, Shyr CR, Meshul CK, Uno H, Platt KA, Chang C. Growth retardation and abnormal maternal behavior in mice lacking testicular orphan nuclear receptor 4. Proc Natl Acad Sci U S A 2004;101:15058–15063
17. Zhang Y, Chen YT, Xie S, Wang L, Lee YF, Chang SS, Chang C. Loss of testicular orphan receptor 4 impairs normal myelination in mouse forebrain. Mol Endo 2007;21:908–920
18. Kim Y-S, Harry GJ, Kang HS, Goulding D, Wine RN, Kissling GE, Liao G, Jetten AM. Altered cerebellar development in nuclear receptor TAK1/TR4 null mice is associated with deficits in GLAST(+) Glia, alterations in social behavior, motor learning, startle reactivity, and microglia. Cerebellum. 2010;9:310–323
19. Liu NC, Lin WJ, Kim E, Collins LL, Lin HY, Yu IC, Sparks JD, Chen LM, Lee YF, Chang C. Loss of TR4 orphan nuclear receptor reduces phosphoenolpyruvate carboxykinase-mediated gluconeogenesis. Diabetes 2007;56:2901–2909
20. Liu NC, Lin WJ, Yu IC, Lin HY, Liu S, Lee YF, Chang C. Activation of TR4 orphan nuclear receptor gene promoter by cAMP/PKA and C/EBP signaling. Endocrine 2009;36:211–217
21. Tanabe O, Shen Y, Liu Q, Campbell AD, Kuroha T, Yamamoto M, Engel JD. The TR2 and TR4 orphan nuclear receptors repress Gata1 transcription. Genes Dev 2007;21:2832–2844
22. Kang HS, Angers M, Beak JY, Wu X, Gimble JM, Wada T, Xie W, Collins JB, Grissom SF, Jetten AM. Gene expression profiling reveals a regulatory role for ROR α and ROR γ in phase I and phase II metabolism. Physiol Genomics 2007;31:281–294
23. Zhou J, Zhai Y, Mu Y, Gong H, Uppal H, Toma D, Ren S, Evans RM, Xie W. A novel pregnane X receptor-mediated and sterol regulatory element-binding protein-independent lipogenic pathway. J Biol Chem 2006;281:15013–15020
24. Erickson SK: Nonalcoholic fatty liver disease. J Lipid Res 2009;50 Suppl:S412–S416
25. Nishino N, Tamori Y, Tateya S, Kawaguchi T, Shibakusa T, Mizunoya W, Inoue K, Kitazawa R, Kitazawa S, Matsuki Y, Hiramatsu R, Masubuchi S, Omachi A, Kimura K, Saito M, Amo T, Ohta S, Yamaguchi T, Osumi T, Cheng J, Fujimoto T, Nakao H, Nakao K, Aiba A, Okamura H, Fushiki T, Kasuga M. FSP27 contributes to efficient energy storage in murine white adipocytes by promoting the formation of unilocular lipid droplets. J Clin Invest 2008;118:2808–2821
26. Zhou Z, Yon Toh S, Chen Z, Guo K, Ng CP, Ponniah S, Lin SC, Hong W, Li P. Cidea-deficient mice have lean phenotype and are resistant to obesity. Nat Genet 2003;35:49–56
27. Keller P, Petrie JT, De Rose P, Gerin I, Wright WS, Chiang SH, Nielsen AR, Fischer CP, Pedersen BK, MacDougald OA. Fat-specific protein 27 regulates storage of triacylglycerol. J Biol Chem 2008;283:14355–14365
28. Silverstein RL, Febbraio M. CD36, a scavenger receptor involved in immunity, metabolism, angiogenesis, and behavior. Sci Signal 2009;2:re3
29. Hallberg M, Morganstein DL, Kiskinis E, Shah K, Kralli A, Dilworth SM, White R, Parker MG, Christian M. A functional interaction between RIP140 and PGC-1α regulates the expression of the lipid droplet protein CIDEA. Mol Cell Biol 2008;28:6785–6795
30. Winer S, Chan Y, Paltser G, Truong D, Tsui H, Bahrami J, Dorfman R, Wang Y, Zielenski J, Mastronardi F, Maezawa Y, Drucker DJ, Engleman E, Winer D, Dosch HM. Normalization of obesity-associated insulin resistance through immunotherapy. Nat Med 2009;15:921–929
31. Guillen N, Navarro MA, Arnal C, Noone E, Arbones-Mainar JM, Acin S, Surra JC, Muniesa P, Roche HM, Osada J. Microarray analysis of hepatic

gene expression identifies new genes involved in steatotic liver. Physiol Genomics 2009;37:187–198
32. Radonjic M, de Haan JR, van Erk MJ, van Dijk KW, van den Berg SA, de Groot PJ, Muller M, van Ommen B. Genome-wide mRNA expression analysis of hepatic adaptation to high-fat diets reveals switch from an inflammatory to steatotic transcriptional program. PLoS One 2009;4:e6646
33. Koonen DP, Jacobs RL, Febbraio M, Young ME, Soltys CL, Ong H, Vance DE, Dyck JR. Increased hepatic CD36 expression contributes to dyslipidemia associated with diet-induced obesity. Diabetes 2007;56:2863–2871
34. Gong J, Sun Z, Li P. CIDE proteins and metabolic disorders. Curr Opin Lipidol 2009;20:121–126
35. Puri V, Ranjit S, Konda S, Nicoloro SM, Straubhaar J, Chawla A, Chouinard M, Lin C, Burkart A, Corvera S, Perugini RA, Czech MP. Cidea is associated with lipid droplets and insulin sensitivity in humans. Proc Natl Acad Sci U S A 2008;105:7833–7838
36. Puri V, Czech MP. Lipid droplets: FSP27 knockout enhances their sizzle. J Clin Invest 2008;118:2693–2696
37. Nagle CA, Klett EL, Coleman RA. Hepatic triacylglycerol accumulation and insulin resistance. J Lipid Res 2009;50(Suppl):S74–S79
38. Vergnes L, Beigneux AP, Davis R, Watkins SM, Young SG, Reue K. Agpat6 deficiency causes subdermal lipodystrophy and resistance to obesity. J Lipid Res 2006;47:745–754
39. Luo J, Sladek R, Carrier J, Bader JA, Richard D, Giguere V. Reduced fat mass in mice lacking orphan nuclear receptor estrogen-related receptor α. Mol Cell Biol 2003;23:7947–7956
40. Leonardsson G, Steel JH, Christian M, Pocock V, Milligan S, Bell J, So PW, Medina-Gomez G, Vidal-Puig A, White R, Parker MG. Nuclear receptor corepressor RIP140 regulates fat accumulation. Proc Natl Acad Sci U S A 2004;101:8437–8442
41. Li L, Xie X, Qin J, Jeha GS, Saha PK, Yan J, Haueter CM, Chan L, Tsai SY, Tsai MJ. The nuclear orphan receptor COUP-TFII plays an essential role in adipogenesis, glucose homeostasis, and energy metabolism. Cell Metab 2009;9:77–87
42. Zhou J, Febbraio M, Wada T, Zhai Y, Kuruba R, He J, Lee JH, Khadem S, Ren S, Li S, Silverstein RL, Xie W. Hepatic fatty acid transporter Cd36 is a common target of LXR, PXR, and PPARγ in promoting steatosis. Gastroenterology 2008;134:556–567
43. Matsusue K, Kusakabe T, Noguchi T, Takiguchi S, Suzuki T, Yamano S, Gonzalez FJ. Hepatic steatosis in leptin-deficient mice is promoted by the PPARγ target gene Fsp27. Cell Metab 2008;7:302–311
44. Shimano H. SREBPs: physiology and pathophysiology of the SREBP family. FEBS J 2009;276:616–621
45. Somm E, Cettour-Rose P, Asensio C, Charollais A, Klein M, Theander-Carrillo C, Juge-Aubry CE, Dayer JM, Nicklin MJ, Meda P, Rohner-Jeanrenaud F, Meier CA. Interleukin-1 receptor antagonist is upregulated during diet-induced obesity and regulates insulin sensitivity in rodents. Diabetologia 2006;49:387–393
46. Somm E, Henrichot E, Pernin A, Juge-Aubry CE, Muzzin P, Dayer JM, Nicklin MJ, Meier CA. Decreased fat mass in interleukin-1 receptor antagonist-deficient mice: impact on adipogenesis, food intake, and energy expenditure. Diabetes 2005;54:3503–3509